Computational Materials Science 51 (2012) 112–116

Contents lists available at SciVerse ScienceDirect

Computational Materials Science

journal homepage: www.elsevier.com/locate/commatsci

Elastic constants of AlB_2-type compounds from first-principles calculations

Y.H. Duan [a,b,*], Y. Sun [a,b], Z.Z. Guo [a,b], M.J. Peng [a,b], P.X. Zhu [a], J.H. He [a,b]

[a] Faculty of Material Science and Technology, Kunming University of Science and Technology, Kunming, Yunnan 650093, PR China
[b] Key Lab of Advanced Materials of Yunnan Province, Kunming University of Science and Technology, Kunming 650093, PR China

ARTICLE INFO

Article history:
Received 16 May 2011
Received in revised form 1 July 2011
Accepted 2 July 2011
Available online 28 August 2011

Keywords:
First principles
Elastic properties
Brittleness
Ductility

ABSTRACT

Elastic constants (C_{ij}'s) of 24 compounds in the AlB_2-type diborides have been calculated by first-principles with the generalized gradient approximation and compared with the available experimental data. Values of all independent elastic constants as well as bulk modulus in *a* and *c* directions (B_a and B_c, respectively) were predicted. The elastic modulus of the AlB_2-type compounds were calculated according to the theoretical elastic constants by Voigt–Reuss–Hill averaging scheme. Ductility and anisotropy in these compounds were further analyzed based on their *B/G* ratio and elastic constants. It is founded that AlB_2 is more ductile while ScB_2 is more brittle, and AlB_2 has a highest elastic anisotropy in the 24 AlB_2-type compounds.

1. Introduction

Magnesium diboride MgB_2, which has been recently founded to be a superconductor with T_c = 39 K by Nagamatsu et al. [1], has a hexagonal AlB_2-type crystal structure (space group P6/*mmm*). B atoms form two-dimensional (2D) honeycomb layers interleaved with Mg ions, in a similar manner to intercalated graphite [2]. MgB_2 and AlB_2 belonging to AlB_2-type compounds have been studied in some detail because of their potential application in electronic devices to overcome current problems of electromigration, corrosion and diffusion into the semiconductor substrate [3–15]. The electronic structure and elastic properties of some hexagonal AlB_2-like diborides had been studied [16–19]. In addition, a set of hypothetical AlB_2-like MB_2 phases (M = Li, Na, Be, Ca, Sr, Ag and Au) was discussed recently, and their properties were analyzed by means of theoretical approaches [20–25]. However, information on the elastic properties of the other AlB_2-type compounds still is scare, such as Actinide and Lanthanide diborides, and so on. In the rapid development of superconductors' and neutron-absorbing materials' field, it is important to investigate the ground-state properties of the AlB_2-type compounds. In the present work elastic constants of AlB_2-type structure compounds (AB_2, A = Al, Cr, Er, Gd, Hf, Lu, Mg, Mn, Mo, Nd, Np, Pu, Sc, Sm, Ta, Tb, Ti, Tm, U, V, W, Y, Yb and Zr) are obtained through first-principles calculations using the efficient stress–strain method [26]. From the results thus obtained, ductility and anisotropy of the compounds are analyzed.

2. Numerical details

The AlB_2-type structure has the AB_2 crystal structure (space group is P6/*mmm*) which is characterized as the coexistence of strong covalent bonding within the honeycomb B layers and metallic bonding between the A and B layers.

The whole researches were carried out through the first principles calculations based on density functional theory (DFT) implemented in Cambridge sequential total energy package (CASTEP) code [27]. Ultrasoft pseudo-potentials were employed to indicate the interactions between ionic core and valence electrons. The exchange correction energies for GGA should be PBE scheme [28]. The Monkhorst–Pack scheme was used for *k* point sampling in the first irreducible Brillouin zone (BZ), and we used $10 \times 10 \times 10$ *k*-point mesh. The maximum cutoff energy was 440.0 eV for plane wave expansions.

There are five independent components of the elasticity tensor for AlB_2-type compounds (C_{11}, C_{12}, C_{13}, C_{33} and C_{44}). The elastic constants are defined by Taylor expansion of the total energy, $E(V, \delta)$, for the system with respect to a small strain δ of the lattice primitive cell volume *V*. The energy of a strained system is expressed as follow [29]:

$$E(V,\delta) = E(V_0,0) + V_0\left[\sum_i \tau_i\xi_i\delta_i + \frac{1}{2}\sum_{ij} C_{ij}\delta_i\xi_j\delta_j\right]. \quad (1)$$

where $E(V_0, 0)$ is the energy of the unstrained system with volume V_0. τ_i is an element in the stress tensor, ξ_i is a factor to Voigt index.

Bulk modulus values are calculated directly within these elastic constants based on the Voigt–Reuss–Hill method (VRH). The formulas for hexagonal crystal class are [30–32]:

* Corresponding author at: Faculty of Material Science and Technology, Kunming University of Science and Technology, Kunming, Yunnan 650093, PR China. Tel.: +86 8715136698.
E-mail address: 19508150@sina.com.cn (Y.H. Duan).

0927-0256/$ - see front matter © 2011 Elsevier B.V. All rights reserved.
doi:10.1016/j.commatsci.2011.07.002

$$B_V = \frac{1}{9}[2(C_{11}+C_{12})+C_{33}+4C_{13}],$$
$$B_R = \frac{(C_{11}+C_{12})C_{33}-2C_{13}^2}{C_{11}+C_{12}+2C_{33}-4C_{13}}, \quad B = \frac{1}{2}(B_V+B_R), \tag{2}$$

The isothermal shear modulus G can be calculated by equation:

$$G_V = \frac{2C_{11}+C_{33}-C_{12}-2C_{13}+6C_{44}+3C_{66}}{15},$$
$$G_R = \frac{15}{4(2S_{11}+S_{33})-4(2S_{13}+S_{12})+3(2S_{44}+S_{66})},$$
$$G = \frac{1}{2}(G_R+G_V), \quad E = \frac{9GB}{G+3B}, \quad v = \frac{3B-E}{6B}, \tag{3}$$

where B, G and E are the bulk modulus, shear modulus and Young's modulus in VRH approximation, respectively; v is Poisson's ratio. B_V (G_V) and B_R (G_R) are determined by the crystal symmetry.

To prove the mechanical anisotropy of AlB_2-type compounds, bulk modulus values along a axis (B_a) and c axis (B_c) can be defined as follows:

$$B_a = a\frac{dp}{da} = \frac{\Lambda}{2+\alpha}, \quad B_c = c\frac{dp}{dc} = \frac{B_a}{\alpha},$$
$$\Lambda = 2(C_{11}+C_{12})+4C_{13}\alpha+C_{33}\alpha^2, \quad \alpha = \frac{C_{11}+C_{12}-2C_{13}}{C_{33}-C_{13}} \tag{4}$$

3. Results and discussions

3.1. Lattice parameters for AlB_2-type compounds

One method to determine the accuracy of the calculations is to compare the calculated lattice parameters with those determined experimentally. Table 1 lists the lattice parameters calculated in comparison with available experimental data [33]. It can be seen that the calculated data show in good agreement with experiments, with the difference being less than 1.5% for all results. The results of equilibrium ratios c/a prove that the compression along c-axis is larger than that along a-axis when the pressure was to be adding. This is consistent with the comparatively weaker bonds (i.e. Al–B bond) which determine the c-axis length. The largest ratio c/a for UB_2 and smallest ratio c/a for VB_2 indicate that the compression of UB_2 and VB_2 are biggest and smallest in AlB_2-type compounds at the same pressure.

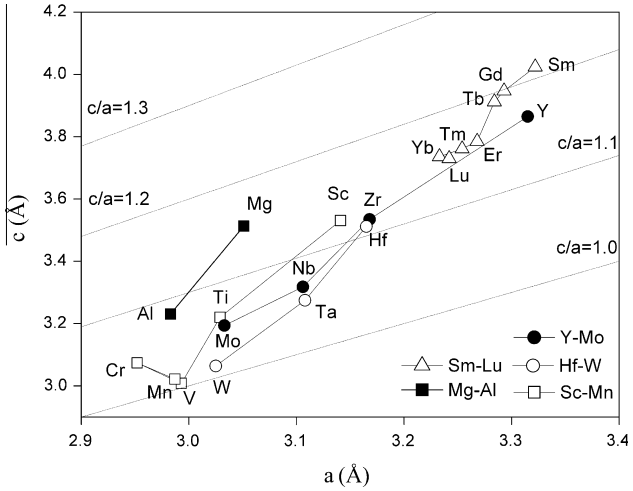

Fig. 1. Calculated lattice parameters of AlB_2-type compounds as a function of valence of A ion.

Table 1 Calculated lattice parameters for AlB_2-type compounds compared with experiments.

By plotting the calculated hexagonal lattice parameters, a and c, and the c/a ratio of AlB_2-type compounds, interesting trends can be found as a function of valence of A ion, as shown in Fig. 1. As the valence increases in a particular period of the Periodic Table except elements U to Pu, the lattice parameters a and c of the AlB_2-type compounds generally decrease and the corresponding c/a ratios also become smaller independent of the period because the variation in c is much larger than that in a.

3.2. Elastic constants

The calculated elastic constants and elastic modulus of 24 AlB_2-type compounds together with their available experimental date [34–36] are shown in Table 2.

Table 1
Calculated lattice parameters for AlB_2-type compounds compared with experiments.

Reference	a (Å)			c (Å)			c/a		
	Calc.	Exp.	%Diff.	Calc.	Exp.	%Diff.	Calc.	Exp.	%Diff.
MgB_2	3.051	3.086	−1.134	3.513	3.521	−0.227	1.151	1.141	0.876
AlB_2	2.983	3.006	−0.765	3.231	3.255	−0.737	1.083	1.083	0
ScB_2	3.141	3.148	−0.222	3.531	3.517	0.398	1.124	1.117	0.627
TiB_2	3.029	3.033	−0.132	3.220	3.231	−0.340	1.063	1.065	−0.188
VB_2	2.993	2.998	−0.167	3.008	3.005	0.100	1.005	1.002	0.299
CrB_2	2.952	2.969	−0.573	3.074	3.066	0.261	1.041	1.033	0.774
MnB_2	2.987	3.009	−0.731	3.022	3.036	−0.461	1.012	1.009	0.297
YB_2	3.315	3.290	0.760	3.865	3.835	0.782	1.166	1.166	0
ZrB_2	3.168	3.165	0.095	3.535	3.533	0.057	1.116	1.116	0
NbB_2	3.106	3.102	0.129	3.318	3.321	−0.090	1.068	1.071	−0.280
MoB_2	3.033	3.005	0.932	3.194	3.173	0.662	1.053	1.056	−0.284
HfB_2	3.165	3.139	0.828	3.512	3.473	1.123	1.110	1.106	0.362
TaB_2	3.108	3.088	0.648	3.275	3.241	1.049	1.054	1.050	0.381
WB_2	3.025	3.020	0.166	3.064	3.050	0.459	1.013	1.010	0.297
SmB_2	3.322	3.310	0.363	4.024	4.019	0.124	1.211	1.214	−0.247
GdB_2	3.293	3.315	−0.664	3.947	3.936	0.279	1.199	1.187	1.011
TbB_2	3.284	3.294	−0.304	3.912	3.886	0.669	1.191	1.180	0.847
ErB_2	3.268	3.271	−0.092	3.785	3.782	0.079	1.158	1.156	0.173
TmB_2	3.254	3.261	−0.215	3.761	3.755	0.160	1.156	1.151	0.434
YbB_2	3.233	3.250	−0.523	3.736	3.732	0.107	1.156	1.148	0.697
LuB_2	3.242	3.244	−0.062	3.730	3.706	0.647	1.151	1.142	0.788
UB_2	3.121	3.136	−0.478	4.002	3.988	0.351	1.282	1.275	0.549
NpB_2	3.148	3.162	−0.443	3.995	3.972	0.579	1.269	1.256	1.035
PuB_2	3.175	3.186	−0.345	3.985	3.949	0.912	1.255	1.239	1.291

Table 2
Calculated elastic constants C_{ij} and elastic modulus of AlB_2-type compounds (in GPa).

Reference	C_{11}	C_{12}	C_{13}	C_{33}	C_{44}	B	B_a	B_c	G	E	v	B/G
MgB_2	434	64	32	278	64	151.5	555.3	313.7	116.4	278.0	0.19	1.30
MgB_2[a]	462	67	41	254	80	157.0	549.6	293.1	125.3	296.9	0.18	1.25
AlB_2	522	75	79	255	32	190.5	778.2	317.6	95	244.4	0.29	2.01
AlB_2[b]	665	41	17	417	58	205.2	734.6	437.3	105.4	269.9	0.28	1.95
ScB_2	487	36	65	366	228	243.8	608.7	464.6	256.6	431.0	0.11	0.95
TiB_2	656	65	98	461	262	250.3	863.7	595.6	260.7	581.0	0.11	0.96
TiB_2[c]	660	48	93	432	260	243.6	851.2	552.8	254.1	565.6	0.11	0.96
VB_2	676	115	130	471	238	279.5	997.0	639.1	240.9	562.2	0.16	1.16
CrB_2	580	184	166	361	160	239.2	1026.3	536.2	139.9	415.4	0.26	1.71
MnB_2	513	217	209	333	109	220.1	1255.5	498.2	121.6	318.4	0.31	1.81
YB_2	359	70	94	329	171	173.5	525.2	509.9	145.3	340.8	0.17	1.19
ZrB_2	557	63	120	437	254	238.6	763.7	636.4	231.4	524.6	0.13	1.03
ZrB_2[d]	581	55	121	445	240	248.0	784.1	642.7	235.2	536.1	0.14	1.05
NbB_2	601	107	185	439	220	286.3	953.9	717.3	210.4	507.0	0.20	1.36
MoB_2	618	130	206	433	169	302.5	1052.8	711.4	186.0	463.1	0.24	1.63
HfB_2	583	98	135	460	257	260.9	852.2	676.3	233.0	538.7	0.16	1.12
TaB_2	597	140	196	433	191	295.8	1022.0	700.0	191.5	472.5	0.23	1.54
WB_2	633	141	241	425	133	322.5	1156.3	727.2	164.1	420.9	0.28	1.97
SmB_2	236	53	75	302	142	128.0	335.0	549.1	110.8	258.0	0.16	1.16
GdB_2	246	55	75	284	131	131.2	354.9	492.9	113.5	264.3	0.16	1.16
TbB_2	252	53	72	289	125	131.3	358.5	484.4	115.4	267.8	0.16	1.14
ErB_2	287	52	73	267	127	137.4	410.5	414.6	119.7	278.3	0.16	1.15
TmB_2	301	52	64	275	123	137.5	421.0	393.5	120.5	279.8	0.16	1.14
YbB_2	334	54	77	301	130	153.7	473.4	425.1	130.2	304.6	0.17	1.18
LuB_2	434	52	72	354	169	178.4	573.6	474.0	173.3	392.7	0.13	1.03
UB_2	352	54	102	492	253	205.5	559.9	777.6	209.5	469.6	0.12	0.98
NpB_2	363	33	93	499	218	206.7	572.3	733.7	169.8	399.3	0.19	1.22
PuB_2	388	30	92	466	230	207.4	600.4	674.6	174.1	408.1	0.17	1.19

[a] Ref. [34].
[b] Ref. [35].
[c] Ref. [36].
[d] Ref. [37].

By plotting the calculated bulk modulus (B) and B_a/B_c as a function of the c/a ratio of AlB_2-type compounds, as shown in Fig. 2, it can be found that, with the c/a ratio increasing, the bulk modulus (B) and the B_a/B_c ratios of the AlB_2-type compounds generally decrease. The declined B_a/B_c ratios with the c/a ratio increasing in Fig. 2b reveal that, longer the c-axis is, closer the compression between along a-axis and along c-axis is. From Fig. 2, it can be seen that the B_a/B_c ratios of the most AlB_2-type compounds are larger than 1 besides Actinide diborides and a few Lanthanide diborides, and the B_a/B_c ratios are less than 1 when the c/a ratio is larger than 1.16. That B_a larger than B_c reveals the compression along a-axis is more difficult than that along c-axis. This phenomenon can be understood by the knowledge of the bonding situations in MgB_2 [38], which are characterized as the coexistence of strong covalent bonding within the honeycomb B layers and metallic bonding between the Mg and B layers. When pressure increases, the atoms in the interlayer become closer, and their interactions become stronger. These mechanical properties imply the anisotropy of MgB_2.

In addition, the B_a/B_c ratios of Lanthanide diborides are up to 1.21 from 0.61, the B_a/B_c ratios of SmB_2, GdB_2, TbB_2 and ErB_2 with smaller atomic number Z are less than 1, while the B_a/B_c ratios of larger Z Lanthanide diborides (TmB_2, YbB_2 and LuB_2) are larger than 1. The B_a/B_c ratios of Actinide diborides and a few Lanthanide diborides are less than 1, in other words, the compression along a-axis is easier than that along c-axis in these AlB_2-type diborides.

To further probe into the mechanical and physical properties of these compounds based on their elastic properties, we analyzed their ductility using the B/G ratio. According to Pugh [39], metals with a B/G ratio greater than 1.75 are ductile whereas metals with a B/G ratio less than 1.75 are considered brittle. Fig. 3 plots the B/G ratio of AlB_2-type compounds against the c/a ratio. As it can be seen in Fig. 3, 3 of the 24 compounds have a B/G ratio greater than 1.75. While AlB_2 has a greatest B/G ratio of 2.01, ScB_2 has the least B/G ratio (0.95). Therefore, it can be ascribed that AlB_2 is more ductile while ScB_2 is more brittle.

3.3. Anisotropy

It is known that the acoustic velocities are related to the elastic constants by Christofell equation [40]. There are two polarizations of the shear waves in elastic waves. For solving the Christofell equation for a hexagonal lattice, one can calculate the anisotropy of the compressional wave (P) as

$$\Delta P = \frac{C_{33}}{C_{11}} \tag{5}$$

For the shear waves, the wave polarized perpendicular to the basal (S_1) and the one polarized in the basal plane (S_2) have the anisotropy,

$$\Delta S_1 = \frac{C_{11} + C_{33} - 2C_{13}}{4C_{44}}, \quad \Delta S_2 = \frac{2C_{44}}{C_{11} - C_{12}}, \tag{6}$$

while for S_2 and P waves the extremum occurs along the c axis, for S_1 it is at an angle of 45° from the c axis in the a–c plane. By plotting the calculated ΔP, ΔS_1, ΔS_2 and the c/a ratio, we illustrated the calculated anisotropy of the compressional wave (ΔP), the shear ΔS_1 (the wave polarized perpendicular to the basal plane S_1), and ΔS_2 (the one polarized in the basal plane S_2) in Fig. 4. Larger the values of ΔP and ΔS_2 are, lower the anisotropy is; and larger the value of ΔS_1 is, higher the anisotropy is. As shown in Fig. 4, it is founded that ΔP, ΔS_1 and ΔS_2 change obviously in the range of c/a ratio. These results may be understood by comparison to an *hcp* crystal interacting with central nearest-neighbor forces (CNNF) [41]. For CNNF model the elastic anisotropy is independent of the interatomic potential to lowest order in P/C_{11}, hence the anisotropy is dependent on the symmetry of the crystal only. In this work, as the valence

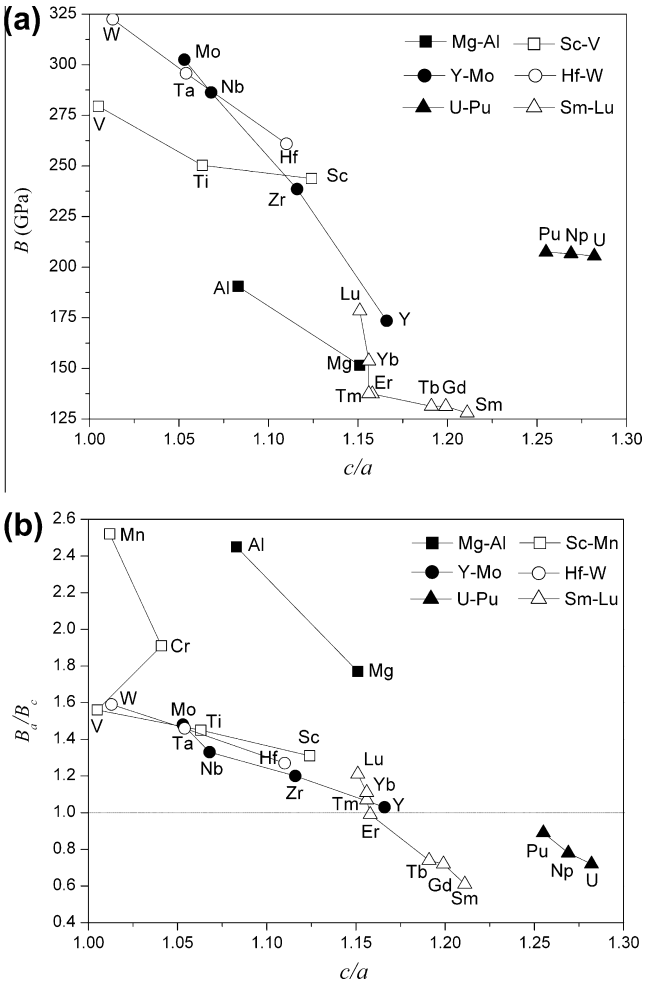

Fig. 2. Calculated B and B_a/B_c of AlB_2-type compounds as a function of c/a ratio.

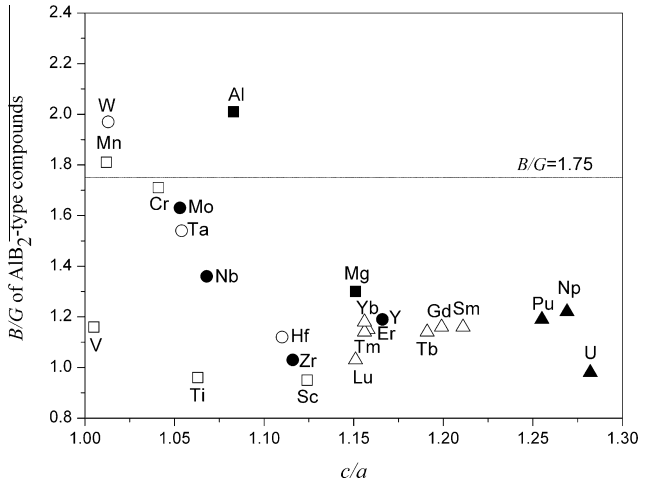

Fig. 3. Ductile/brittle properties of AlB_2-type compounds based on elastic properties.

increases in a particular period of the Periodic Table, we found the ratios c/a of AlB_2-type compounds decrease, that is, the symmetry lower and cause to the higher elastic anisotropy. From Fig. 4, AlB_2 has the highest elastic anisotropy in the 24 AlB_2-type compounds.

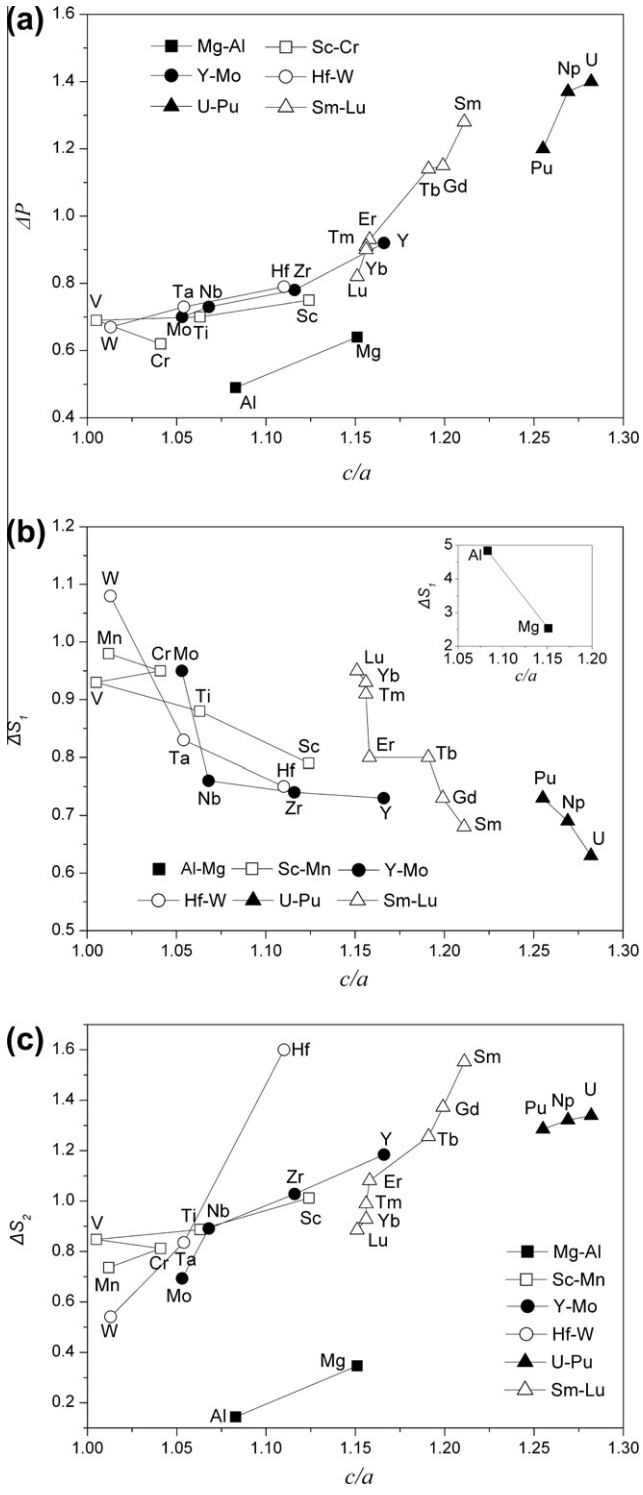

Fig. 4. As a measure of anisotropy the elastic constant ratios C_{33}/C_{11}, $(C_{11}+C_{33}-2C_{13})/4C_{44}$ and $2C_{44}/(C_{11}-C_{12})$, which govern the compressional (ΔP) and shear wave anisotropy (ΔS_1 and ΔS_2, respectively) of AlB_2-type compounds, are shown as a function of the ratios c/a.

4. Conclusions

Elastic constants of 24 AlB_2-type compounds have been calculated from first-principles within the generalized gradient approximation correction (GGA) in the frame of density functional theory. The elastic properties of these compounds have been correlated to their ductility and anisotropy, thereby providing an understanding

for their deformation behavior. Analysis of the calculated parameters reveals some of AlB_2-type compounds with high anisotropy are ductile. AlB_2 has the highest elastic anisotropy and it is more ductile in the 24 AlB_2-type compounds.

Acknowledgments

This work was supported by the National Natural Science Foundation of China under Grant No. 50871049 and National High-Tech Research and Development Program of China (863 Program) under Grant No. 2009AA03Z512. First-principles' calculations were carried out at Key Lab of Advance Materials in Rare & Precious and Nonferrous Metals, Ministry of Education, China.

References

[1] J. Nagamatsu, N. Nakagawa, T. Muranaka, Y. Zenitani, J. Akimistu, Nature 410 (2001) 63–64.
[2] T. Oguchi, J. Phys. Soc. Jpn. 71 (2002) 1495–1500.
[3] R.J. Cava, Nature 410 (2001) 23–24.
[4] D.C. Larbalestier, L.D. Cooley, M.O. Rikel, A.A. Polyanskil, J. Jiang, S. Patnaik, X.Y. Cai, D.M. Feldmann, A. Gurevich, A.A. Squitieri, M.T. Naus, C.B. Eom, E.E. Hellstrom, R.J. Cava, K.A. Regan, N. Rogado, M.A. Hayward, T. He, J.S. Slusky, P. Khalifah, K. Inumaru, M. Hass, Nature 410 (2001) 186–189.
[5] P.C. Canfield, D.K. Finnermore, S.L. Bud'ko, J.E. Ostenson, G. Lapertot, C.E. Cunningham, C. Petrovic, Phys. Rev. Lett. 86 (2001) 2423–2426.
[6] I.I. Mazin, V.P. Antropov, Physica C 385 (2003) 49–65.
[7] J. Fjellstedt, A.E.W. Jarfors, L. Svendsen, J. Alloy Compd. 283 (1999) 192.
[8] M. Nakao, Physica C 388–389 (2003) 137.
[9] K.P. Bohnen, R. Heid, B. Renker, Phys. Rev. Lett. 86 (2001) 5771–5774.
[10] R. Heid, B. Renker, H. Schober, P. Adelmann, D. Ernst, K.P. Bohnen, Phys. Rev. B 67 (2003) 180510.
[11] N.I. Medvedeva, A.L. Ivanovskii, J.E. Medvedeva, A.J. Freeman, Phys. Rev. B 64 (2001) 020502.
[12] B. Fisher, K.B. Chashka, L. Patlagan, G.M. Reisner, Physica C 384 (2003) 1–10.
[13] J. Kortus, I.I. Mazin, K.D. Belashchenko, V.P. Andropov, L.L. Boyer, Phys. Rev. Lett. 86 (2001) 4656–4659.
[14] I. Loa, K. Kunc, K. Syassen, P. Bouvier, Phys. Rev. B 66 (2002) 134101.
[15] A.K.M.A. Islam, F.N. Islam, Physica C 363 (2001) 189–193.
[16] I.R. Shein, A.L. Ivanovskii, J. Phys.: Condens. Matter 20 (2008) 415218.
[17] J.K. Burdett, E. Canadell, G.J. Miller, J. Am. Chem. Soc. 108 (1986) 6561–6568.
[18] X.B. Wang, D.C. Tian, L.L. Wang, J. Phys.: Condens. Matter 6 (1994) 10185.
[19] J.L. Wang, Z. Zeng, Q.Q. Zheng, Physica C 408–410 (2004) 264–265.
[20] A.L. Ivanovskii, Phys. Solids State 45 (2003) 1829–1859.
[21] J. Akimitsu, S. Akutagawa, K. Kawashima, T. Muranaka, Prog. Theor. Phys. Suppl. 159 (2005) 326.
[22] J. Kortus, Physica C 456 (2007) 54–62.
[23] G. Satta, G. Profeta, F. Bernardini, A. Continenza, S. Massidda, Phys. Rev. B 64 (2001) 104507.
[24] P. Ravindran, P. Vajeeston, R. Vidya, A. Kjekshus, H. Fjellvag, Phys. Rev. B 64 (2001) 224509.
[25] K. Kobayashi, M. Arai, K. Yamamoto, Mater. Transact. 47 (2006) 2629.
[26] S. Shang, Y. Wang, Z.K. Liu, Appl. Phys. Lett. 90 (2007) 101909.
[27] M.D. Segall, P.J.D. Lindan, M.J. Probert, C.J. Pickard, P.J. Hasnip, S.J. Clark, M.C. Payne, J. Phys.: Condens. Matter 14 (2002) 2717–2744.
[28] M. Marlo, V. Milman, Phys. Rev. B 62 (2000) 2899–2907.
[29] L. Fast, J.M. Wills, B. Johansson, O. Eriksson, Phys. Rev. B 51 (1995) 17431–17438.
[30] W. Voigt, Lehrbuch der Kristallphysik, Taubner, Leipzig, 1928.
[31] A. Reuss, Z. Angew, Math. Mech. 9 (1929) 49–58.
[32] R. Hill, Proc. Phys. Soc. A 65 (1952) 349–354.
[33] P. Vallars, Pearson's Handbook: Crystallographic Data for Intermetallic Phases, ASM International, Materials Park, OH, 1997.
[34] H.Y. Wang, X.R. Chen, W.J. Zhu, Y. Cheng, Phys. Rev. B 72 (2005) 172502.
[35] K. Liu, X.L. Zhou, X.R. Chen, W.J. Zhu, Physica B 388 (2007) 213–218.
[36] P.S. Spoor, J.D. Maynard, M.J. Pan, D.J. Green, J.R. Hellmann, T. Tanaka, Appl. Phys. Lett. 70 (1997) 1959–1961.
[37] K.B. Panda, K.S. Ravi Chandran, Comput. Mater. Sci. 35 (2006) 134–150.
[38] J.M. Osorio-Guillén, S.I. Simak, Y. Wang, B. Johansson, R. Ahuja, Solid State Commun. 123 (2002) 257–262.
[39] S.F. Pugh, Philos. Mag. 45 (1954) 823–843.
[40] H.Y. Wang, Y. Cheng, X.R. Chen, Q.Q. Guo, Commun. Theor. Phys. 45 (2006) 558–564.
[41] M. Born, K. Huang, Dynamical Theory of Crystal Lattices, Oxford, Clarendon, 1954.